JACS
JOURNAL OF THE AMERICAN CHEMICAL SOCIETY

Article

pubs.acs.org/JACS

Homochiral and *meso* Figure Eight Knots and a Solomon Link

Nandhini Ponnuswamy,[†,§] Fabien B. L. Cougnon,[†,§] G. Dan Pantoş,*[,†,‡] and Jeremy K. M. Sanders*[,†]

[†]University Chemical Laboratory, University of Cambridge, Lensfield Road, CB2 1EW, Cambridge, U.K.

[‡]Department of Chemistry, University of Bath, BA 7AY, Bath, U.K.

Supporting Information

ABSTRACT: A homochiral naphthalenediimide-based building block forms in water a disulfide library of macrocycles containing topological isomers. We attempted to identify each of these isomers, and explored the mechanisms leading to their formation. The two most abundant species of the library were assigned as a topologically chiral Solomon link (60% of the library, as measured by high-performance liquid chromatography (HPLC)) and a topologically achiral figure eight knot (18% by HPLC), competing products with formally different geometries but remarkably similar 4-fold symmetries. In contrast, a racemic mixture of building blocks gives the near-quantitative formation of another new and more stable structure, assigned as a *meso* figure eight knot. Taken together, these results seem to uncover a correlation between the point chirality of the building block used and the topological chirality of the major structure formed. These and the earlier discovery of a trefoil knot also suggest that the number of rigid components in the building block may translate into corresponding knot symmetry and could set the basis of a new strategy for constructing complex topologies.

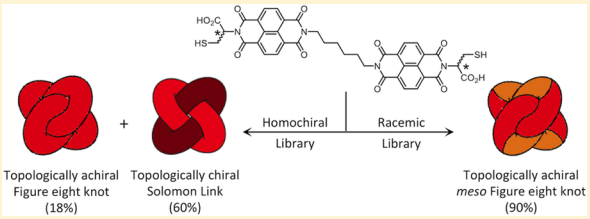

Over the last several decades, the structures of natural molecular knots and links[1−3] have inspired research chemists to devise ingenious synthetic strategies for creating abiotic molecular knots.[4,5] Since the stepwise and kinetically controlled synthesis of the first molecular trefoil knot by Sauvage,[6] molecules with higher order topologies—Solomon links,[7−15] Borromean links,[16] pentafoil knots,[17] and composite knots[18]—have been successfully accessed by exploiting metal-ion-templated reversible assembly from simple building blocks. In spite of these significant advances, designing suitable ligands remains challenging, and the synthesis of molecular topologies with more than three crossings has only rarely been achieved.

We recently described the dynamic assembly in water of a dithiol building block into a molecular trefoil knot,[19] the formation of which is driven by the need to produce a structure that sequesters the hydrophobic surfaces of the building block from the aqueous environment.[20] The results presented here suggest that the same driving force can be harnessed as a general strategy in knot synthesis. We report the discovery of three new structures, which appear to be a Solomon link and two closely related figure eight knots. The latter structures are particularly exciting because the figure eight knot topology, identified in a natural protein, plant acetohydroxy acid isomeroreductase,[21] has previously only been synthesized using a DNA scaffold.[22] Notwithstanding chemists' extensive efforts, mostly through the groups of Walba,[23] Fenlon,[24] and Sauvage,[25] the synthesis of non-DNA-based molecular figure eight knots has remained elusive. Importantly, the Solomon link and the figure eight knot exhibit remarkably similar 4-fold symmetries (D4 or S4). However, in contrast with the Solomon link, which is topologically chiral and can be either right-handed or left-handed, the figure eight knot is a topologically achiral structure.[26−31]

RESULTS AND DISCUSSION

1. Identification of Topologically Different Macrocycles in a Single Library. The LL building block depicted in Figure 1 is composed of two identical hydrophobic π-systems (1,4,5,8-naphthalenediimide, NDI) connected via a flexible 1,6-hexylene linker and terminated by two L-cysteine moieties that provide chirality, reactive thiols, and hydrophilic carboxylates.[32] A disulfide library was generated by dissolving the building block in water at pH 8 at a concentration of 5 mM and was stirred at room temperature under air in capped vials for 1 day to allow slow oxidation of the thiols. Tandem liquid chromatography-mass spectrometry (LC-MS) analysis of the library after full oxidation (Figure 2a) revealed the presence of the dimer (at 23 min), trimer (at 29 min), and four tetramers (**1**, **2**, **3**, and **4**). Larger macrocycles were not observed, probably due to entropic and kinetic factors.

The presence of four fully oxidized (m/z 1639.6, doubly charged), and therefore cyclic, tetramers eluting at different retention times (at 19, 20, 27, and 34 min, respectively) suggests that they are distinct topological isomers.[33] A tetramer can be in the form of either a single macrocyclic component, which can be knotted, or a molecular link composed of two or more interlocked macrocycles. In order to assign the topology corresponding to each of the tetramers, we first built all the possible structures using a CPK model. From the many

Received: December 11, 2013
Published: May 15, 2014

   dx.doi.org/10.1021/ja4125884 | *J. Am. Chem. Soc.* 2014, 136, 8243−8251

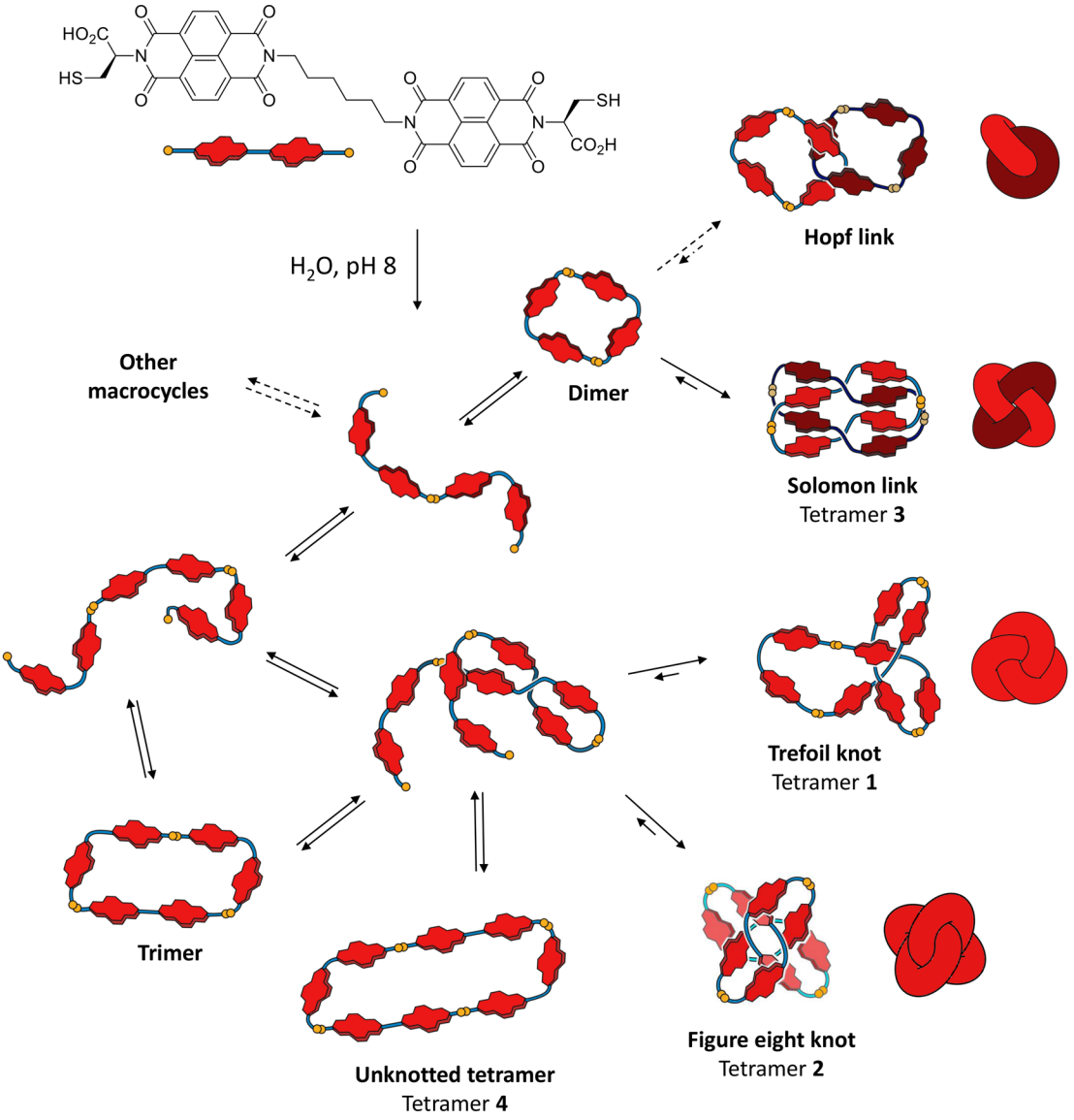

Figure 1. Topological isomers that can form in a disulfide library generated from one single chiral LL building block (derived from L-cysteine). The red components of the cartoons represent the naphthalenediimide units, and the yellow dots represent the sulfur atoms connecting the building blocks.

topologies defined by mathematicians (Figure S2, Supporting Information), only the simplest topologies, drawn in Figure 1, could be constructed. The steric constraints imposed by the rigid NDI components of the building block allow no more than four crossings, limiting the accessible structures of the knots to the simple macrocycle (the unknot with no crossing), the trefoil knot (three crossings), and the figure eight knot (four crossings). Similarly, the structures of the links are limited to the singly interlocked [2]catenane (two crossings, the Hopf link) and the doubly interlocked [2]catenane (four crossings, the Solomon link). More complex structures, such as the Whitehead link, composite knots, pentafoil knot, or the Star of David, could not be constructed due to steric strain.

We attempt below to assign each of the accessible topologies shown in Figure 1 by the concerted use of mass spectrometry (MS) and 1D and 2D nuclear magnetic resonance (NMR) and circular dichroism (CD) spectroscopies. This approach is supported by evidence accumulated from closely related and homologous[19,32] NDI-based disulfide libraries. In these systems, *flexible* NDI-based macrocycles typically exhibited weak CD signals because of the lack of fixed geometrical relationships among the macrocyles' constituent parts, which results in the averaging of exciton coupling interactions. This relative flexibility also results in broad NMR signals at 298 K, due to slow tumbling on the NMR chemical shift time scale; the NMR signals sharpens with increased temperature and faster tumbling. On the other hand, *tightly interlocked* NDI-based macrocycles with well-defined geometries exhibit intense CD signals and temperature-independent sharp NMR spectra that reflect the symmetry of the structure.

Tetramer 4: the Unknot? High-performance liquid chromatography (HPLC) elution of the cyclic dimer, trimer, and tetramer typically occurs in succession based on ring size. However, links or knots show a relatively lower retention time compared to the flexible trivial macrocycles, because their hydrophobic surfaces are efficiently buried by folding or packing and their hydrophilic surfaces are exposed.[19,32] Relative values of HPLC retention time in a homologous series can

dx.doi.org/10.1021/ja4125884 | J. Am. Chem. Soc. 2014, 136, 8243−8251

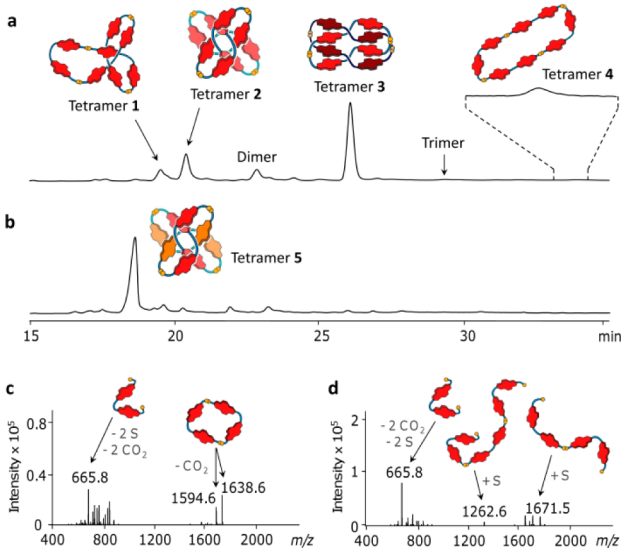

Figure 2. LC-MS analysis of the libraries in water at pH 8. (a) 5 mM library of the chiral building block (derived from L-cysteine), highlighting the presence of four tetrameric species (**1**, **2**, **3**, and **4**). (b) 5 mM library of a racemic mixture of building blocks (LL building block in shades of red, DD building block in orange). The cartoons represent the topologies assigned to each of the tetramers. Absorbance was recorded at 383 nm. (c) MS/MS fragmentation of tetramer **3**. (d) MS/MS fragmentation of tetramer **1**. The MS/MS fragmentation of tetramers **2**, **4**, and **5** is identical to that of tetramer **1**.

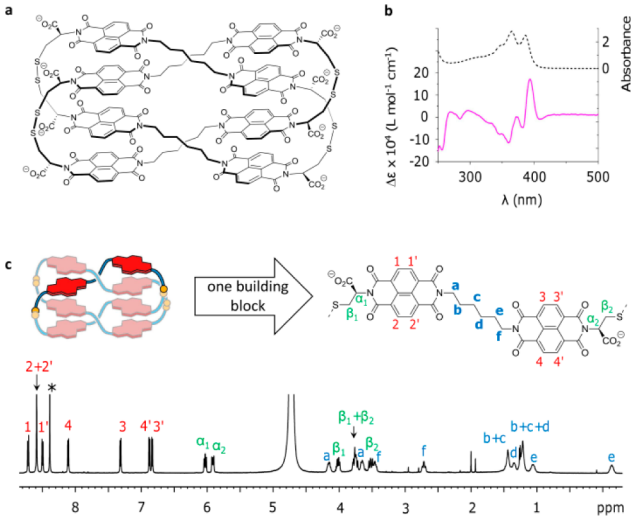

Figure 3. Characterization of tetramer **3**. (a) Proposed topology as a Solomon link. (b) UV–vis (dashed line) and CD spectra (pink line) of the Solomon link in water at 298 K. (c) ^{1}H NMR spectrum (500 MHz, D_2O, 298 K). Residual formic acid, introduced during the purification process, is labeled with a star.

therefore be used as a preliminary indication of compactness. On the basis of HPLC, the tetramer **4**, with the longest retention time, is more likely to be the unknot, a hypothesis strengthened by its MS/MS fragmentation pattern, characteristic of a noncatenated macrocycle (Figure 2d).[32,34] Tetramer **4** is only observed in trace amounts, which implies that its formation is unfavorable, presumably because it has a flexible structure that cannot efficiently hide its hydrophobic surfaces from the aqueous environment. Unfortunately, the low yield of formation of **4** prevented its isolation for further characterization. Its assignment as an unknotted macrocycle therefore remains tentative.

On the other hand, tetramers **1**, **2**, and **3** are formed in significant proportion and have remarkably shorter retention times, typical of the compact structures of interlocked and folded molecules.[19,32] Tetramers **1**, **2**, and **3** were isolated by preparative HPLC in milligram quantities and were further characterized by NMR and CD spectroscopies (Figure S3, Supporting Information).

*Tetramer **3**: a Solomon Link?* The MS/MS analysis revealed that the most abundant species of the library (60% of the library, estimated from the HPLC peak area), tetramer **3**, fragments exclusively into a dimer (m/z 1638.6, singly charged) and smaller fragments, and is therefore composed of two interlocked dimers (Figure 2c). On the basis of the accessible topologies presented in Figure 1, it can either be the rigid Solomon link or the more flexible, but tightly folded, Hopf link.

Tetramer **3** exhibits a sharp ^{1}H NMR spectrum (500 MHz, 298 K, D_2O) and displays an intense induced CD signal, consisting of a positive band in the NDI absorption region (385 nm) and a negative band in the imide region (250 nm, Figure 3). In accordance with precedent,[32] the Hopf link should unfold at higher temperatures or upon addition of a less polar solvent such as acetonitrile, and exhibit significant variations in ^{1}H NMR or CD. However, no noteworthy changes in the NMR and the CD signatures were observed upon increasing the temperature (from 298 to 348 K, Figures S4 and S10, Supporting Information) or modifying the solvent polarity (from 0 to 25% of acetonitrile in water at 298 K, Figures S5 and S11, Supporting Information) with the exception of trivial variations of the chemical shifts of some NDI protons.

The occurrence of highly shielded NDI proton signals (chemical shift <7 ppm) indicates the presence of closely packed NDI moieties. The large number of NOE cross-peaks observed between the NDI and aliphatic protons (Figure S8, Supporting Information) strengthen the argument that **3** has a compact structure, in which aromatic cores and aliphatic chains are in close proximity. These observations, indicative of a molecule with little flexibility, suggest that tetramer **3** is more likely to be the more organized of the two structures proposed, which is the Solomon link. Furthermore, the diffusion coefficient of tetramer **3** measured by DOSY is 2.3×10^{-10} m^2/s (after calibrating the d_6-acetone/D_2O diffusion). At 298 K, assuming the molecule to be spherical, this corresponds to a volume of 2.9×10^{-27} m^3 which is in close agreement with the volume of the Solomon link estimated by molecular modeling calculations (Table S2, Supporting Information).

The Solomon link is more rigid than the Hopf link because of the higher number of crossings, and molecular dynamics calculations[35] further illustrate these relative rigidities. Calculations on both links were performed at different temperatures using either Amber99 or Charmm27 force fields in a water dielectric medium, using a completely stacked conformation as a starting point (Figure S43, Supporting Information). Both at 343 and 363 K, the stacked conformation of the Hopf link converts into a very loose and open conformation, showing that the energy barrier required by the Hopf link to undergo conformational changes is readily surmounted at the temperatures investigated (Table S3, Supporting Information). In sharp contrast, no change in the conformation of the Solomon link is observed at either temperature, showing that conformational motion is prevented by unfavorable/high-energy steric clashes (Figure S46, Supporting Information).

dx.doi.org/10.1021/ja4125884 | J. Am. Chem. Soc. 2014, 136, 8243–8251

Analysis of the ^{1}H NMR spectrum of **3** discloses its 4-fold symmetry, with an equivalent environment for each of the four building blocks composing the structure, wherein every proton of an individual building block is inequivalent. The spectrum at 298 K displays eight doublets in the NDI region (9.4 to 7.6 ppm) corresponding to each NDI proton of one building block: four upfield-shifted (inner protons) and four downfield-shifted (outer protons, Figure S6, Supporting Information). The aliphatic protons buried within the hydrophobic core are observed as diastereotopic pairs spanning a wide range of chemical shifts from 4.2 to −0.2 ppm. This NMR spectrum is consistent with a compact, rigid, and 4-fold symmetrical molecule. The structure of the Solomon link, with a D_4 symmetry point, perfectly fits these observations.

The succession of the aliphatic protons can be traced by using 2D COSY, as illustrated in Figure 5a: the diastereotopic protons display COSY cross-peaks with one another (solid lines) and cross-peaks with *J*-coupled neighboring protons (dashed lines). The observation that the right- and left-hand sides of the aliphatic chain, and of the whole building block, are not equivalent demonstrates the presence of an inherent directionality, implying that the topology of **3** is chiral. Indeed, the Solomon link is an intrinsically chiral topology, and **3** may exist in two diastereomeric forms, *P* and *M*.

Only one diastereomer of the Solomon link is observed by NMR, indicating that its synthesis is stereoselective, with the chirality of the L-cysteine dictating the topological chirality of the link. Among all the topologies drawn in Figure 1, the Solomon link is the only one that fits all the MS, NMR, and CD data observed for tetramer **3**, giving us a high confidence in our interpretation. The molecular dynamic simulations provide further support.

Tetramer 2: a Figure Eight Knot? The same reasoning applied to tetramer **2**, which has an MS/MS spectrum characteristic of a noncatenated species (Figure 2d), suggests a trefoil, a figure eight knot, or an unknotted structure. Most of the NMR signals are sharp (Figure 4c) and remain sharp upon increasing the temperature (from 278 to 317 K) or adding acetonitrile (from 0 to 30%), suggesting a compact and well-organized structure (Figures S13 and S14, Supporting Information). As previously, the ^{1}H NMR spectrum of tetramer **2** implies a 4-fold symmetry. The compactness and the symmetry of **2** are not consistent with the asymmetric and relatively loose trefoil knot or the flexible unknotted macrocycle. In contrast, the figure eight knot is a compact molecule that possesses a 4-fold symmetry[30] (S4), as depicted in Figure 1.

As illustrated in Figure 4c, the S4 symmetry of the figure eight knot would imply that **2** is composed of four identical arms. We identified the two sets of α-cysteine protons, overlapping in D_2O but distinguishable upon addition of acetonitrile (Figure S14, Supporting Information). Four sets of *J*-coupled NDI protons were also identified by 2D COSY at 333 K between 9.2 and 7.4 ppm, due to the presence of two NDI rings in different environments (Figure S15, Supporting Information). While most NDI resonances of **2** are sharp, a few are broad (notably protons 2′, 4, and 4′, Figure 4c) and undergo significant sharpening upon increasing the temperature, implying a range of available NDI chemical environments.

2D COSY and 2D NOESY analysis of the aliphatic protons of the hexylene chain revealed the presence of two inequivalent linkers (in red and blue, Figure 5b). Each linker possesses a center of symmetry located in its middle, implying that the right- and left-hand sides of each building block are now

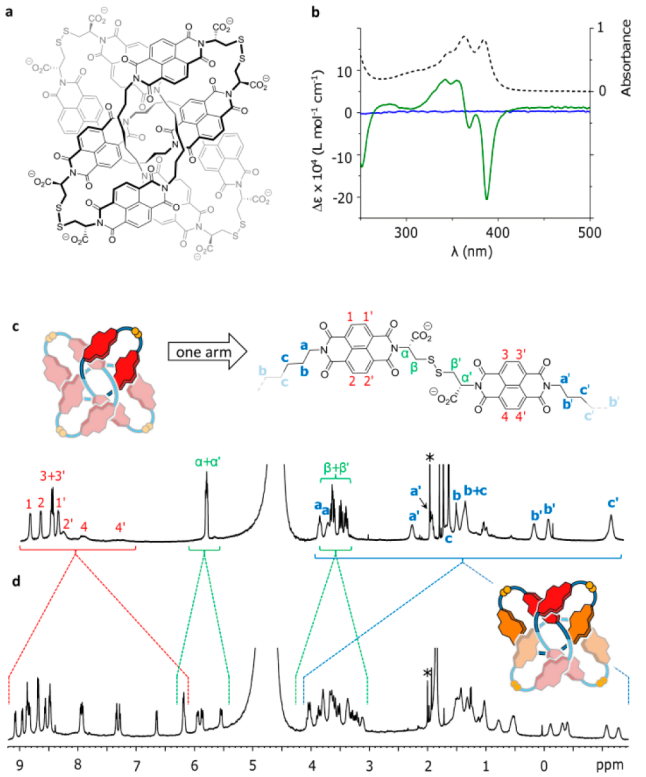

Figure 4. Characterization of tetramers **2** and **5**. (a) Proposed chemical structure of tetramer **2** (homochiral figure eight knot). (b) UV−vis (dashed line) and CD spectra of **2** (homochiral, green line) and **5** (*meso*, blue line) knot in water at 298 K. (c) ^{1}H NMR spectrum (500 MHz, D_2O, 298 K) of **2** (the homochiral knot). (d) ^{1}H NMR spectrum (500 MHz, D_2O, 298 K) of **5**, the proposed *meso* LL-DD-LL-DD knot. Residual acetic acid, introduced during the purification process, is labeled with a star.

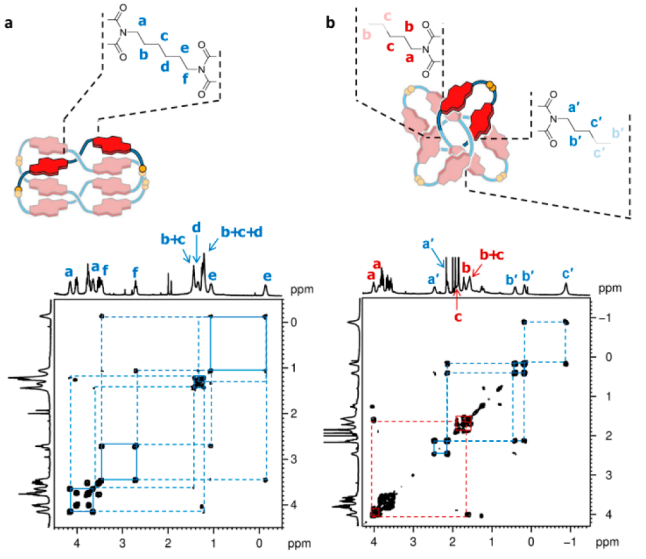

Figure 5. Comparison between the 2D correlations observed for the aliphatic chains of (a) tetramer **3** (the Solomon link) and (b) tetramer **2** (the homochiral figure eight knot). Cross-peaks corresponding to diastereotopic protons are shown in solid lines and cross-peaks with *J*-coupled neighboring protons in dashed lines.

dx.doi.org/10.1021/ja4125884 | *J. Am. Chem. Soc.* 2014, 136, 8243−8251

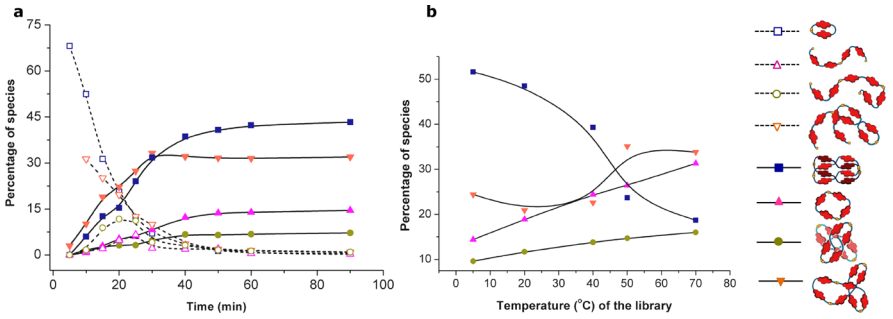

Figure 6. Kinetics of formation of knots and links, and effect of temperature. (a) Kinetic profile of a library (5 mM, water pH 8), showing the consumption of the building block and the formation of the molecules assigned as being the Solomon link, the trefoil knot, and the figure eight knot. The formation and disappearance of the intermediates can also be traced: open dimer, closed dimer, open trimer, and open tetramer. Trace amounts of the closed trimer and the unknotted tetramer could not be quantified. The percentages were determined from the HPLC peak areas (absorption monitored at 383 nm). (b) Variation of the library distribution at different temperatures.

equivalent and do not possess any directionality of the kind seen in the topologically chiral Solomon link **3**.

Such a unique and symmetric pattern of COSY cross-peaks is unlikely to fit a tightly folded unknotted macrocycle, and is perfectly consistent with the achiral topology of the figure eight knot, where the aliphatic protons are buried in the core of the molecule, while the hydrophilic cysteines are located on the outer surface, pointing outward.

In spite of its achiral topology, molecule **2** is homochiral (because of the presence of eight L-cysteines). It is a rigid twisted molecule with a high symmetry that renders the exciton couplings additive, leading to a strong CD signal (Figure 4b), independent of temperature and of medium polarity (Figures S19 and S20, Supporting Information). It is notable that tetramer **3** and tetramer **2** display opposite CD maxima, presumably arising from the different geometrical relationships between the NDIs in the two interlocked structures.

To conclude, the high degree of symmetry and the lack of directionality only seem to fit, among all the topologies drawn in Figure 1, the S4 figure eight knot, a chemically homochiral LL-LL-LL-LL molecule with an achiral topology.

Tetramer 1: a Trefoil Knot? Finally, through a process of elimination, the last tetramer (**1**), which also fragments as a noncatenated macrocycle, is probably the trefoil knot. The disparity between the 2-fold symmetry of the building block and the 3-fold symmetry of the trefoil knot is likely to produce a flexible yet compact multiconformational molecule that lacks symmetry, in agreement with the broad ^{1}H NMR resonances and the weak CD signal intensity observed (Figures S22 and S23, Supporting Information). As a consequence of the broad NMR, no further solution-based analysis can support our hypothesis that **1** is a trefoil knot.

Summary. From the five topologies accessible with a CPK model, we were able to identify four topologies of the same tetrameric macrocycle within one single library. We believe that the experimental results and thorough analysis presented here strongly support our assignment of **3** being a Solomon link and **2** a figure eight knot. Our assignments of **1** as a trefoil knot and **4** as the unknotted macrocycle remain tentative, but their presence would fit a common mechanism of formation described below (Figure 1). We believe that the Hopf link is not significantly present in this library, as explained below. In order to facilitate the reading of the following parts, tetramers **1**−**4** will be referred to using the name of the topology to which they have been assigned.

2. Exploration of the Kinetic Pathways Leading to Either the Solomon Link or the Figure Eight Knot. The Solomon link (tetramer **3**) and the figure eight knot (tetramer **2**) are likely to be the thermodynamic products of this library, based upon their abundance and their favorable packed structures, as supported by the data described earlier. Notably, these structures are formed at the expense of what one might assume to be the entropically less demanding trefoil knot (tetramer **1**), thus highlighting the influence of symmetry in the formation of these species.

In order to determine the kinetic profile of the library, we monitored the oxidation of a 5 mM library by LC-MS at intervals of 5 min (Figure S27, Supporting Information). The kinetic results presented in Figure 6, in agreement with the mechanism proposed in Figure 1, indicate the operation of two distinct pathways: the threading of a closed dimer by an open dimer leading to the formation of the Solomon link and the knotting of the open tetramer resulting in the formation of the figure eight knot. The faster formation of the dimeric species explains why the Solomon link appears before the figure eight knot, which is derived from the open tetramer, a species with slower evolution.

Each of these intricate structures represents a kinetic trap that is likely to accumulate in the library over time. Interconversion between these fully oxidized structures would involve the cleavage of a disulfide link followed by the unfolding of the oligomeric species, which requires an unfavorable re-exposure of hydrophobic surfaces. The residual presence of the trefoil knot fits into our mechanistic considerations. Indeed, folding of the open tetramer may lead either to the trefoil or to the figure eight knot. The trefoil knot has a simpler topology, with three crossings instead of four, and could form as a kinetic product. It is more flexible and may not cover its hydrophobic surfaces as efficiently as the figure eight, but once it is formed, a high energy barrier of unfolding may render its reorganization into the more stable figure eight knot too slow within the oxidation time frame of the library.

Following a similar reasoning, we would expect to find the Hopf link in the library. The absence of the Hopf link may indicate its low stability and rapid conversion into the Solomon link. This observation may be explained by the fact that the Hopf link is the structure with the fewer number of crossings (two), and its unfolding into dimeric species cannot be excluded. As mentioned above, molecular dynamics calculations show that the Solomon link is more compact than the Hopf link and that the most populated conformation of the Hopf link

dx.doi.org/10.1021/ja4125884 | J. Am. Chem. Soc. 2014, 136, 8243−8251

suffers from a much larger solvent-exposed hydrophobic surface, which is expected to lead to a lower thermodynamic stability. Further molecular dynamics studies (Amber99, water dielectric medium at 343 K) on the structures resulting from threading once (Hopf) or twice (Solomon) an open dimer through a closed dimer (pseudo-Hopf and pseudo-Solomon links) were performed. These calculations showed that, regardless of its initial folding state, the pseudo-Hopf link readily dethreads to form the open and closed dimers as individual species. Under identical conditions, no dethreading was observed for the pseudo-Solomon link (Figure S47−S50, Supporting Information).

While the library composition evolves over a few hours, the formation of the Solomon link and of the figure eight knot occurs mostly within the first 40 min of oxidation, which is significantly faster than the several hours necessary to produce any of the simpler interlocked structures (Hopf link[32] or trefoil knot[19]) previously reported by our group from similar aqueous dynamic combinatorial systems. This observation leads us to consider that increasing the topological complexity might not necessarily correlate to an increase in the energy barrier controlling the folding pathway. The formation of more complex architectures from simple organic units may not be as challenging as previously thought: it only depends on the appropriate choice of the building block.

3. Effect of Temperature on the Library Distribution. We determined the effect of various stimuli on the library distribution, such as pH, addition of inorganic salt, and temperature (Figures S25 and S26, Supporting Information). While it is difficult to rationalize the effect of temperature on such complex systems,[36] especially on the kinetics of folding into either a link or knot, Figure 6b highlights a correlation between the increase in yield of the dimer and the decrease in yield of the Solomon link, with an intersection point at about 318 K, suggesting that the two species are linked through a common mechanism of formation. On the other hand, both the yield of the trefoil knot and the figure eight knot concomitantly increase with temperature. A kinetic experiment, run at 343 K (Figures S28 and S29, Supporting Information), suggests that the increase in yield of the figure eight knot (from 15% at 278 K to 33% at 343 K) might be due, at least partly, to an increase in the rate of oligomerization that could favor the formation of the open tetramer and, as a result, of the knotted macrocycles.

4. Synthesis of a New Structure, Tetramer 5: a *meso* Figure Eight Knot. Moving from one building block (a single enantiomer) that gives a relatively simple library to the racemic mixture can lead *either* to self-sorting into a racemic mixture of the already most stable accessible structure (e.g., racemic mixture of the right- and left-handed molecule)[19] *or* to an improved yield of a thermodynamically even more stable structure. Indeed, preparing a library with a racemic mixture has occasionally led to the formation of more stable *meso* macrocycles containing both enantiomeric building blocks.[37] We therefore prepared a racemic library containing equimolar amounts of the LL and DD homochiral building blocks.[38]

While the formation of any of the topologies described above should still be possible, preparation of the racemic library almost exclusively led to the formation of one species, **5** (90% yield by HPLC, m/z 1639.6, doubly charged, Figure 2b). MS/MS shows that **5** is a noncatenated tetramer: it could therefore be an unknot, a trefoil knot, or a figure eight knot. The new product was isolated by preparative HPLC and further analyzed by NMR (Figure S30, Supporting Information).

In accord with the reasoning developed above, the sharp NMR signals of tetramer **5** in D_2O at 298 K (Figure 4d) immediately reveal that the new molecule has a highly organized structure with a 2-fold symmetry. The presence of strongly shielded protons, both in the NDI (up to 6.3 ppm) and in the aliphatic (up to −1.5 ppm) regions, corroborates that these protons are buried within the hydrophobic core of a compact molecule. The previous analysis of the homochiral library suggests that, among the three possible topologies, these features are characteristic of a figure eight knot.

This new figure eight knot could either be composed of a LL-DD-DD-DD, LL-LL-DD-DD, or LL-DD-LL-DD sequence of building blocks (Figure S31, Supporting Information). These three structures are diastereomers and should be differentiable by HPLC and NMR, as previously demonstrated in the case of other topologies.[32] The presence of one single HPLC peak supports the assignment of tetramer **5** as a single diastereomer and only the LL-DD-LL-DD figure eight knot, with C_2 point symmetry (Figure S41, Supporting Information), fits the 2-fold symmetry exhibited by the ^{1}H NMR. Molecular modeling calculations also support that the ground state energy of a *meso* figure eight knot is the lowest for the LL-DD-LL-DD conformation (Table S4, Supporting Information).

In the new *meso* LL-DD-LL-DD knot, two adjacent arms are inequivalent, while opposite arms are equivalent (Figure 4d). The NMR signals observed should therefore correspond to two full arms of the molecule. Indeed, the NMR spectrum displays 16 doublets in the NDI region (9.0 to 6.3 ppm) corresponding to four different NDIs, four α-protons for the cysteines, and two aliphatic linkers (Figures S37 and S38, Supporting Information).

A diffusion coefficient of 2.0×10^{-10} m^2/s was measured for the *meso* knot **5** at 298 K, corresponding to a volume of 2.6×10^{-27} m^3, assuming the molecule to be spherical (Figure S40, Supporting Information). It is therefore slightly smaller than the homochiral knot **2** (diffusion coefficient, 2.5×10^{-10} m^2/s; volume, 3.2×10^{-27} m^3; Figure S18, Supporting Information), an observation in agreement with both the lower retention time (18 min versus 21 min) and higher yield of formation (90% versus 18% at 298 K) of **5**. Compared to the homochiral knot **2**, the *meso* knot **5** also exhibits significantly sharper NMR signals at 298 K, and some signals more shielded (chemical shifts <1 ppm), which was interpreted as reflecting a perfect fit between the achiral topology of the figure eight knot and its *meso* backbone (LL-DD-LL-DD). Using a similar reasoning, the comparative broadness of the ^{1}H NMR signals of the homochiral knot may reflect an inherent mismatch between the topological achirality of the knot and the homochirality of its backbone (LL-LL-LL-LL).

Stereochemistry and Molecular Motion of the Figure Eight **5**. Figure 7a shows homochiral figure eight knots **2**, tied in one direction or in the opposite direction (**2A** and **2B**). A simple rotation by 90° immediately reveals that the two knots are actually identical.

In contrast, the loss of the 4-fold symmetry in the *meso* knot NMR spectrum implies that **5A** and **5B** are non-superimposable, and are therefore enantiomers (Figure 7b). Importantly, the two enantiomers are interconvertible, as pulling the backbone of **5A** converts it into **5B**.

Although two enantiomers have identical NMR spectra, the exchange can be traced by 2D exchange spectroscopy EXSY,[39] because it also corresponds to the exchange between the two adjacent, and inequivalent, arms of the knot (Figure 8). A

dx.doi.org/10.1021/ja4125884 | J. Am. Chem. Soc. 2014, 136, 8243−8251

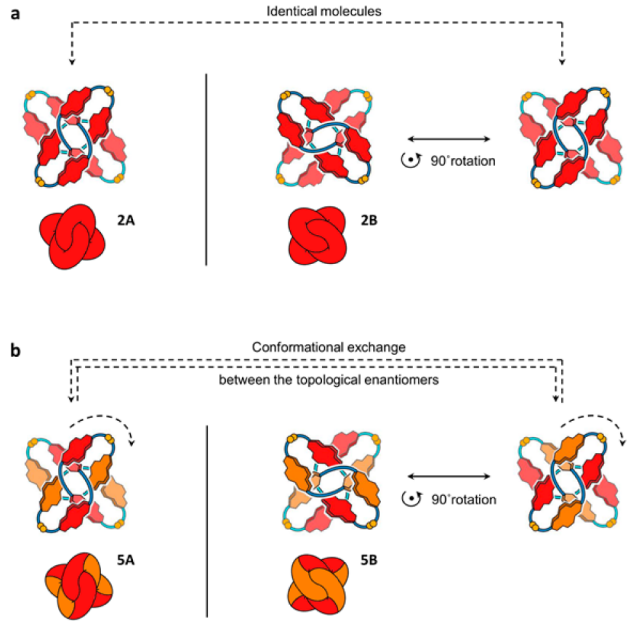

Figure 7. Right- and left-handed *meso* LL-DD-LL-DD figure eight knots (tetramer **5**) are enantiomers. (a) Tying the homochiral figure eight knot **2** in one direction or in the other direction results in identical molecules. (b) Tying the LL-DD-LL-DD *meso* figure eight knot **5** in one direction or in the other direction results in non-superimposable knots (enantiomers) that can exchange through conformational motion along the knot backbone.

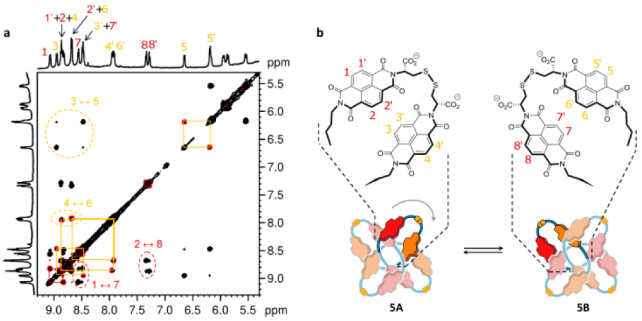

Figure 8. 2D exchange spectroscopy of the *meso* LL-DD-LL-DD figure eight knot (tetramer **5**). (a) The exchange signals observed by NOESY (500 MHz, D_2O, 298 K, d_8 = 200 ms) fit the pattern expected for (b) the interconversion between the two enantiomeric knots. Pulling the knot backbone results in the motion of the top-right arm to the adjacent position (top-left).

repetitive pattern of exchange signals was observed between each pair of NDI protons in the 2D NOESY. The activation enthalpy ($\Delta H^{\ddagger}$ = −21 kJ mol^{-1}) and entropy ($\Delta S^{\ddagger}$ = −302 J K^{-1} mol^{-1}) and the energy barrier ($\Delta G^{\ddagger}$ = +69 kJ mol^{-1} at 298 K) of conversion were determined by monitoring the temperature dependence of the relative intensity of the exchange peaks (Figure S39, Supporting Information). The favorable enthalpy of activation may be explained by the electrostatic repulsion between the closely packed NDIs, which is released in the transition state. In contrast, the large penalty associated with the activation entropy indicates a highly constrained transition state in which the buried hydrophobic surfaces become exposed to the solvent. The activation parameters suggest that the hydrophobic effect not only governs the synthesis but also the conformational motion of the proposed *meso* figure eight knot **5**.

Kinetics of Formation of Tetramer ***5***. The formation of the proposed *meso* figure eight knot **5** is significantly slower (2 h) than that of the proposed homochiral figure eight knot **2** (40 min), presumably because it is situated in a more complex energy landscape involving the formation of many homo and heterochiral intermediates (open dimer, trimer, and tetramer), few of which have the right sequence of building blocks (Figures S42 and S43, Supporting Information). The absence of any of the homochiral species previously observed highlights the higher stability of the new knot. Because all the possible knots and links are kinetic traps and should accumulate over time, even if formed in a relatively low yield, the absence of any other species also suggests that the formation of the intermediates with alternating chiralities, such as the open LL-DD-LL-DD tetramer, is favored over the formation of the other intermediates, such as the homochiral LL-LL-LL-LL tetramer.

5. Emerging Elements of Design. The formation of knots and links involves a delicate balance between the entropic gain generated by the number of water molecules released from the desolvation of hydrophobic groups and the entropic cost of assembling building blocks into a knotted structure, which has fewer degrees of freedom because of its rigidity.

An efficient synthesis of these structures necessitates an optimum packing of the NDI cores and of the aliphatic units. Optimum packing arises from a good match between the individual building blocks and the overall structure, in terms of symmetry and chirality: we previously reported that a building block containing three NDI units leads to a 3-fold symmetrical knot,[19] while analogues incorporating two NDI units produce a 2-fold symmetrical Hopf link.[32] In both cases, entropy favors the formation of the simplest interlocked structures, the Hopf link or the trefoil knot, preventing the formation of the higher order structures.

The results presented above suggest that the construction of more complex structures does not necessarily require the synthesis of more complex building blocks. By introducing a small difference in the building block containing two NDIs previously used and by reducing its flexibility, we inhibited the assembly of a Hopf link, allowing the formation of the immediately higher order structures with a symmetry multiple of two: the 4-fold symmetrical Solomon link and figure eight knot (Figure 9).

There also seems to be a correlation between the chirality of the building block used and the topological chirality of the final structure. Chiral structures, such as the trefoil knot or the Solomon link, necessitate the use of homochiral building blocks (all-L or all-D). They are stereoselectively assembled and self-sort on using a racemic mixture of building blocks. On the other hand, achiral structures, such as the figure eight knot, are selected when a racemic mixture of building blocks is used.

■ CONCLUSIONS

Many molecules with complex topologies can be produced from one simple symmetrical building block, limiting the synthetic cost of the final architectures and simplifying their characterization. In the absence of X-ray diffraction data, we have attempted to assign the topology of the species formed in a system with a high degree of complexity, by using a rigorous method based on the combination of complementary analytical techniques and on symmetry analysis.[19,40] The formation of the knots and links reported by our group supports the existence of a relationship between the structure of the building blocks and

dx.doi.org/10.1021/ja4125884 | J. Am. Chem. Soc. 2014, 136, 8243−8251

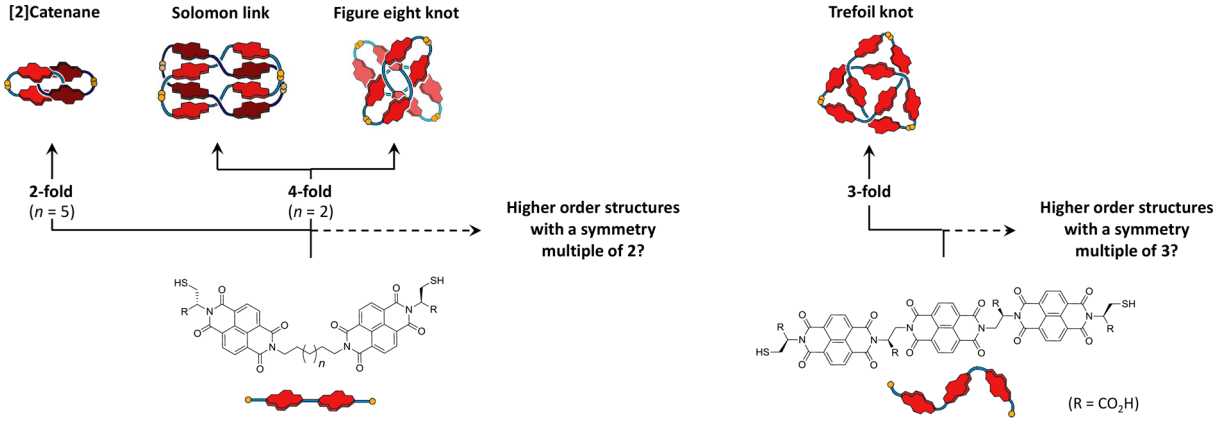

Figure 9. A possible relationship between the number of rigid components in the building block and the symmetry of the interlocked structure (link or knot) formed in water from naphthalenediimide-based building blocks. The chirality of the building blocks also affects the topological chirality of the resulting structure.

that of the topology ultimately formed. Introducing the elements of symmetry and chirality described here in the design of building blocks composed of alternating hydrophobic/hydrophilic and rigid/flexible units may ultimately enable us to encode the information necessary for their folding into molecules with a particular topology.

■ ASSOCIATED CONTENT

Supporting Information

Detailed procedure for building block synthesis, library preparations, HPLC/LC-MS methods and data, UV−vis, CD, and NMR spectra of isolated molecules, and molecular modeling calculations. This material is available free of charge via the Internet at http://pubs.acs.org.

■ AUTHOR INFORMATION

Corresponding Authors

g.d.pantos@bath.ac.uk
jkms@cam.ac.uk.

Author Contributions

[§]N.P. and F.B.L.C. contributed equally.

Notes

The authors declare no competing financial interest.

■ ACKNOWLEDGMENTS

We are grateful to Gates Cambridge (N.P.), EPSRC (F.B.L.C., J.K.M.S.), and the University of Bath (G.D.P.) for financial support. We thank Dr. Ana Belenguer for maintaining the LC-MS facility. We are grateful to Prof. Erica Flapan of Pomona College for helpful discussions regarding symmetry and topology.

■ REFERENCES

(1) Liu, L. F.; Perkocha, L.; Calender, R.; Wang, J. C. *Proc. Natl. Acad. Sci. U.S.A.* **1981**, *78*, 5498−5502.
(2) Liang, C. Z.; Mislow, K. *J. Am. Chem. Soc.* **1994**, *116*, 11189−11190.
(3) Virnau, P.; Mallam, A. L.; Jackson, S. E. *J. Phys.: Condens. Matter* **2011**, *23*, 033101.
(4) Forgan, R. S.; Sauvage, J.-P.; Stoddart, J. F. *Chem. Rev.* **2011**, *111*, 5434−5464.
(5) Ayme, J.-F.; Beves, J. E.; Campbell, C. J.; Leigh, D. A. *Chem. Soc. Rev.* **2013**, *42*, 1700−1712.
(6) Dietrich-Buchecker, C. O.; Sauvage, J.-P. *Angew. Chem., Int. Ed. Engl.* **1989**, *28*, 189−192.
(7) Nierengarten, J.-F.; Dietrich-Buchecker, C. O.; Sauvage, J.-P. *J. Am. Chem. Soc.* **1994**, *116*, 375−376.
(8) Dietrich-Buchecker, C.; Sauvage, J.-P. *Chem. Commun.* **1999**, 615−616.
(9) Ibukuro, F.; Fujita, M.; Yamaguchi, K.; Sauvage, J.-P. *J. Am. Chem. Soc.* **1999**, *121*, 11014−11015.
(10) McArdle, C. P.; Vittal, J. J.; Puddephatt, R. J. *Angew. Chem., Int. Ed.* **2000**, *39*, 3819−3822.
(11) McArdle, C. P.; Jennings, M. C.; Vittal, J. J.; Puddephatt, R. J. *Chem.—Eur. J.* **2001**, *7*, 3572−3583.
(12) Peinador, C.; Blanco, V.; Quintela, J. M. *J. Am. Chem. Soc.* **2009**, *131*, 920−921.
(13) Pentecost, C. D.; Chichak, K. S.; Peters, A. J.; Cave, G. W. V.; Cantrill, S. J.; Stoddart, J. F. *Angew. Chem., Int. Ed.* **2007**, *46*, 218−222.
(14) Beves, J. E.; Campbell, C. J.; Leigh, D. A.; Pritchard, R. G. *Angew. Chem., Int. Ed.* **2013**, *52*, 6464−6467.
(15) Prakasam, T.; Lusi, M.; Elhabiri, M.; Platas-Iglesias, C.; Olsen, J.-C.; Asfari, Z.; Cianférani-Sanglier, S.; Debaene, F.; Charbonnière, L. J.; Trabolsi, A. *Angew. Chem., Int. Ed.* **2013**, *52*, 9956−9960.
(16) Chichak, K. S.; Cantrill, S. J.; Pease, A. R.; Chiu, S.-H.; Cave, G. W. V.; Atwood, J. L.; Stoddart, J. F. *Science* **2004**, *304*, 1308−1312.
(17) Ayme, J.-F.; Beves, J. E.; Leigh, D. A.; McBurney, R. T.; Rissanen, K.; Schultz, D. *Nat. Chem.* **2011**, *4*, 15−20.
(18) Carina, R. F.; Dietrich-Buchecker, C.; Sauvage, J.-P. *J. Am. Chem. Soc.* **1996**, *118*, 9110−9116.
(19) Ponnuswamy, N.; Cougnon, F. B. L.; Clough, J. M.; Pantoş, G. D.; Sanders, J. K. M. *Science* **2012**, *338*, 783−785.
(20) Corbett, P. T.; Leclaire, J.; Vial, L.; West, K. R.; Wietor, J.-L.; Sanders, J. K. M.; Otto, S. *Chem. Rev.* **2006**, *106*, 3652−3711.
(21) Biou, V.; Dumas, R.; Cohen-Addad, C.; Douce, R.; Job, D.; Pebay-Peyroula, E. *EMBO J.* **1997**, *16*, 3405−3415.
(22) Seeman, N. C. *Angew. Chem., Int. Ed.* **1998**, *37*, 3220−3238.
(23) Walba, D. M.; Zheng, Q. Y.; Schilling, K. *J. Am. Chem. Soc.* **1992**, *114*, 6259−6260.
(24) Fenlon, E. E.; Ito, B. R. *Eur. J. Org. Chem.* **2008**, 3065−3068.
(25) Dietrich-Buchecker, C.; Sauvage, J.-P. *New. J. Chem.* **1992**, *16*, 271−285.
(26) Walba, D. M. *Tetrahedron* **1985**, *41*, 3161−3212.
(27) Fenlon, E. E. *Eur. J. Org. Chem.* **2008**, 5023−5035.
(28) Liang, C.; Mislow, K. *J. Math. Chem.* **1994**, *15*, 1−34.
(29) Liang, C.; Mislow, K. *J. Math. Chem.* **1994**, *15*, 245−260.
(30) (a) Flapan, E. *When Topology meets Chemistry: A Topological Look at Molecular Chirality*; Cambridge University Press: New York, 2000. (b) Flapan, E.; Seeman, N. C. *J. Chem. Soc., Chem. Commun.* **1995**, 2249−2250.
(31) Chambron, J.-C.; Sauvage, J.-P.; Mislow, K. *J. Am. Chem. Soc.* **1997**, *119*, 9558−9559.

(32) Cougnon, F. B. L.; Ponnuswamy, N.; Jenkins, N. A.; Pantoş, G. D.; Sanders, J. K. M. *J. Am. Chem. Soc.* **2012**, *134*, 19129−19135.
(33) Another hypothesis is that the four tetramers observed correspond to the same macrocycle locked into different conformations, potentially because of the macrocycle binding to a guest. However, the isolated products do not re-equilibrate into the whole library when dissolved in D_2O, even at high temperature, suggesting that the difference of energy between the conformations would be considerable. Both our MS and NMR data do not account for guest binding. Finally, we prepared libraries from analogous building blocks with linkers varying from ethylene to nonylene (see the Supporting Information). Only the hexylene linker produced the four tetramers: the other libraries were only composed of the monomer and the dimer in various ratios. This observation suggests that a specific geometry is necessary for the formation of the four tetramers, strengthening our hypothesis that they are different topologies.
(34) Schill, G. *Catenanes, Rotaxanes and Knots*; Academic Press: 1971.
(35) (a) Stewart, J. J. P. *J. Mol. Model.* **2007**, *13*, 1173−1213. (b) Korth, M. *J. Chem. Theory Comput.* **2010**, *6*, 3808−3816. (c) Klamt, A.; Schüürmann, G. *J. Chem. Soc., Perkin Trans. 2* **1993**, *2*, 799−805.
(36) Otto, S.; Engberts, J. B. F. N. *Org. Biomol. Chem.* **2003**, *1*, 2809−2820.
(37) Corbett, P. T.; Tong, L. H.; Sanders, J. K. M.; Otto, S. *J. Am. Chem. Soc.* **2005**, *127*, 8902−8903.
(38) The behavior of the LD building block, containing an L-cysteine on one side and a D-cysteine on the other side, has not been investigated.
(39) Pons, M.; Millet, O. *Prog. Nucl. Magn. Reson. Spectrosc.* **2001**, *38*, 267−324.
(40) For other examples of related structural determinations using NMR, see: (a) Wietor, J.-L.; Pantoş, G. D.; Sanders, J. K. M. *Angew. Chem., Int. Ed.* **2008**, *47*, 2689−2692. (b) Engelhard, D. M.; Freye, S.; Grohe, K.; John, M.; Clever, G. H. *Angew. Chem., Int. Ed.* **2012**, *51*, 4747−4750.